



Myogenic tone is impaired at low arterial pressure in mice deficient in the low-voltage-activated Cav3.1 T-type Ca²⁺ channel

Björling, K.; Morita, H.; Olsen, M. F.; Prodan, A.; Hansen, P. B.; Lory, P.; von Holstein-Rathlou, Niels-Henrik; Jensen, Lars Jørn

Published in:
Acta Physiologica (Print)

DOI:
[10.1111/apha.12066](https://doi.org/10.1111/apha.12066)

Publication date:
2013

Document version
Publisher's PDF, also known as Version of record

Citation for published version (APA):
Björling, K., Morita, H., Olsen, M. F., Prodan, A., Hansen, P. B., Lory, P., von Holstein-Rathlou, N-H., & Jensen, L. J. (2013). Myogenic tone is impaired at low arterial pressure in mice deficient in the low-voltage-activated Ca_v3.1 T-type Ca²⁺ channel. *Acta Physiologica (Print)*, 207(4), 709-720. <https://doi.org/10.1111/apha.12066>

Myogenic tone is impaired at low arterial pressure in mice deficient in the low-voltage-activated $\text{Ca}_v3.1$ T-type Ca^{2+} channel

K. Björling,¹ H. Morita,² M. F. Olsen,¹ A. Prodan,^{1*} P. B. Hansen,^{3†} P. Lory,⁴ N.-H. Holstein-Rathlou⁵ and L. J. Jensen¹

¹ Department of Veterinary Clinical and Animal Sciences, Faculty of Health and Medical Sciences, University of Copenhagen, Denmark

² Special Patient Oral Care Unit, Kyushu University Hospital, Fukuoka, Japan

³ Department of Cardiovascular and Renal Research, Institute of Molecular Medicine, University of Southern Denmark, Odense, Denmark

⁴ CNRS, Institut de Génomique Fonctionnelle, Université de Montpellier, France

⁵ Department of Biomedical Sciences, Faculty of Health and Medical Sciences, University of Copenhagen, Denmark

Received 31 October 2012,
revision requested 27 December 2012,

accepted 17 January 2013

Correspondence: Department of Veterinary Clinical and Animal Sciences, Grønnegaardsvej 7, Frederiksberg, Copenhagen DK-1870, Denmark

E-mail: Lajj@sund.ku.dk

*Present address: A. Prodan, Department of Oral Biochemistry, Academic Centre for Dentistry Amsterdam (ACTA), Amsterdam, the Netherlands.

†P.B. Hansen was supported by grants from the Danish Medical Research Council (11-107552)

Abstract

Aim: Using mice deficient in the $\text{Ca}_v3.1$ T-type Ca^{2+} channel, the aim of the present study was to elucidate the molecular identity of non-L-type channels involved in vascular tone regulation in mesenteric arteries and arterioles.

Methods: We used immunofluorescence microscopy to localize $\text{Ca}_v3.1$ channels, patch clamp electrophysiology to test the effects of a putative T-type channel blocker NNC 55-0396 on whole-cell Ca^{2+} currents, pressure myography and Ca^{2+} imaging to test diameter and Ca^{2+} responses of the applied vasoconstrictors, and Q-PCR to check mRNA expression levels of several Ca^{2+} handling proteins in wild-type and $\text{Ca}_v3.1^{-/-}$ mice.

Results: Our data indicated that $\text{Ca}_v3.1$ channels are important for the maintenance of myogenic tone at low pressures (40–80 mm Hg), whereas they are not involved in high-voltage-activated Ca^{2+} currents, Ca^{2+} entry or vasoconstriction to high KCl in mesenteric arteries and arterioles. Furthermore, we show that NNC 55-0396 is not a specific T-type channel inhibitor, as it potently blocks L-type and non-L-type high-voltage-activated Ca^{2+} currents in mouse mesenteric vascular smooth muscle cell.

Conclusion: Our data using mice deficient in the $\text{Ca}_v3.1$ T-type channel represent new evidence for the involvement of non-L-type channels in arteriolar tone regulation. We showed that $\text{Ca}_v3.1$ channels are important for the myogenic tone at low arterial pressure, which is potentially relevant under resting conditions *in vivo*. Moreover, $\text{Ca}_v3.1$ channels are not involved in Ca^{2+} entry and vasoconstriction to large depolarization with, for example, high KCl. Finally, we caution against using NNC 55-0396 as a specific T-type channel blocker in native cells expressing high-voltage-activated Ca^{2+} channels.

Keywords arteriolar tone, $\text{Ca}_v3.1$ T-type channel, mesenteric artery, myogenic response, voltage-gated calcium channel.

Voltage-gated Ca^{2+} channels are encoded by 10 different genes and are divided into the high-voltage-activated Ca^{2+} channels, to which the L-type, P/Q-type, N-type and R-type belong, and the low-voltage-activated Ca^{2+} channels to which the T-type channels belong (Catterall *et al.* 2003). In vascular smooth muscle cells (VSMCs), the L-type channels are important for excitation–contraction coupling and therefore have a dominant role in arteriolar tone regulation, blood pressure regulation and hypertension (Nelson *et al.* 1990, Pratt *et al.* 2002, Moosmang *et al.* 2003). However, the contribution of non-L-type channels to vascular tone regulation is of potential clinical relevance because a proportion of vasospasms in the coronary and cerebral circulations are resistant to treatment with L-type Ca^{2+} antagonists (Beltrame *et al.* 2004, Oshima *et al.* 2005, Fukumoto *et al.* 2008, Velat *et al.* 2011). Furthermore, coronary blood flow, endothelial function and renal function in hypertensive subjects show significant improvement after treatment with combined L- and T-type channel blockers (Beltrame *et al.* 2004, Oshima *et al.* 2005, Koh *et al.* 2007, Sasaki *et al.* 2009). Recently, the expression of $\text{Ca}_v3.1$ and $\text{Ca}_v3.2$ T-type Ca^{2+} channels was demonstrated in small arteries and arterioles from the rat mesenteric (Gustafsson *et al.* 2001, Jensen *et al.* 2004, Braunstein *et al.* 2009), cremasteric (VanBavel *et al.* 2002), renal (Hansen *et al.* 2001) and cerebral (Kuo *et al.* 2010) circulations. Because the expression of L-type channels and the effect of L-type channel blockers were shown to be reduced in the most peripheral branches of the mesenteric circulation (Morita *et al.* 1999, 2002, Gustafsson *et al.* 2001, Jensen *et al.* 2004), it was suggested that the T-type channels are especially important for tone regulation in the most peripheral resistance vessels of the systemic circulation (Gustafsson *et al.* 2001, Jensen *et al.* 2004, Ball *et al.* 2009). Recombinant T-type channels are low-voltage-activated and undergo rapid voltage-dependent inactivation at depolarized potentials more positive than -50 mV (Perez-Reyes 2003). Nevertheless, previous studies in rat mesenteric resistance vessels have shown that high-voltage-activated whole-cell Ca^{2+} currents and Ca^{2+} entry to high KCl in VSMCs, which were resistant to L-type channel blockade using nifedipine, were highly sensitive to several T-type channel blockers, such as mibefradil, NiCl_2 , pimozone, ethosuximide, NNC 55–0396 and R(-)-efonidipine (Morita *et al.* 2002, Jensen *et al.* 2004, Braunstein *et al.* 2009). In rat mesenteric arterioles, P/Q-type channels were not expressed and the Ca^{2+} entry to high KCl was not blocked by highly specific peptide toxin inhibitors of P/Q-type, N-type or R-type channels (Jensen *et al.* 2004). It was therefore speculated that a splice variant of T-type channels is expressed in mesenteric resistance vessels which activate and mediate Ca^{2+} entry via

non-inactivating window currents at membrane potentials more depolarized than the hyperpolarized potentials at which recombinant pore-forming subunits of the $\text{Ca}_v3.1$ channels are activated (Jensen & Holstein-Rathlou 2009).

Myogenic tone is associated with a near-linear relationship between intraluminal pressure and depolarization of VSMCs in intact cerebral and skeletal muscle arteries, going from a membrane potential of approx. -60 mV at low pressure (20–40 mm Hg) to approx. -30 mV at high pressure (100–120 mm Hg) (Knot & Nelson 1998, Kotecha & Hill 2005). L-type channel splice variants in smooth muscle cells show non-inactivating window currents in the voltage range from -55 to -10 mV (Liao *et al.* 2007), and Ca^{2+} entry through L-type channels is known to be important for maintaining myogenic tone in resistance vessels (Davis & Hill 1999). Recombinant $\text{Ca}_v3.1$ T-type Ca^{2+} channels are activated and inactivated at relatively more hyperpolarized membrane potentials than are L-type channels, and their activation and inactivation curves overlap at more hyperpolarized membrane potentials in the range between -65 and -55 mV, thus giving rise to a small, non-inactivating window current in this voltage range (Monteil *et al.* 2000). We therefore speculated that a non-inactivating Ca^{2+} influx is activated at low pressures in mouse mesenteric VSMCs due to window currents through $\text{Ca}_v3.1$ T-type channels. However, conclusive studies have been hampered by the lack of specific T-type channel blockers, although some recent studies suggested that the compounds NNC 55–0396 and R(-)-efonidipine are T-type specific (Furukawa *et al.* 2004, Huang *et al.* 2004). Recently, transgenic mice born with a deletion of either the $\text{Ca}_v3.1$ (Kim *et al.* 2001) or the $\text{Ca}_v3.2$ (Chen *et al.* 2003) T-type Ca^{2+} channels have become available. Using mice deficient in the $\text{Ca}_v3.1$ T-type channel, the aim of the present study was therefore to elucidate the molecular identity of non-L-type channels involved in vascular tone regulation in mesenteric arteries and arterioles by comparing the vasoconstrictor effects of (i) an increase in intraluminal pressure, (ii) application of a depolarizing KCl-containing solution and (iii) exposure of the vessels to physiological concentration of noradrenaline. This study is relevant for clarifying the contribution of T-type channels to vascular tone regulation in mesenteric arteries and arterioles, which had previously been prevented by the lack of specific T-type antagonists.

Materials and methods

Animals and tissue preparations

Studies were conducted using $\text{Ca}_v3.1^{-/-}$ mice and weight- and age-matched C57BL/6J mice (Taconic Farm Inc., Lille Skensved, Denmark). Mice knockout

for the $\text{Ca}_v3.1$ T-type Ca^{2+} channel ($\text{Ca}_v3.1^{-/-}$), originally developed in HS Shin's laboratory (Kim *et al.* 2001), were backcrossed for more than 10 generations to the C57BL/6J genetic background. Genotyping was performed as described previously (Kim *et al.* 2001). The mice of both genotypes were 5–8-month-old males and weighed 26–39 g. There were no clinical signs or dysfunction due to $\text{Ca}_v3.1$ deletion or age. Mice were killed immediately before use by cervical dislocation. The intestines were quickly removed and submersed in oxygenated (95% O_2 /5% CO_2) Krebs buffer at room temperature. Second- or third-order mesenteric arteries (<200 μm lumen) were quickly removed using sharpened forceps and ophthalmic scissors under a stereo microscope (Leica M80; Leica Microsystems, Wetzlar, Germany) with cold light illumination (Leica CLS150XE; Leica Microsystems, Wetzlar, Germany), and used for pressure myography, Q-PCR and immuno-fluorescence microscopy. Mesenteric terminal arterioles (<40 μm lumen) were excised from the fat pads adjacent to the border of the ileum as previously described (Braunstein *et al.* 2009) and used for Ca^{2+} imaging experiments. For whole-cell patch clamp electrophysiology, 10–11-week-old Sprague Dawley rats ($N = 10$) and 9–12-week-old C57BL/6J mice ($N = 4$) of either sex were used. These rats and mice were anaesthetized by exposure to sevoflurane and killed by cervical dislocation, and small mesenteric arteries (<200 μm) were excised and used for isolation of single VSMCs. This study conforms to good publication practice in physiology (Persson & Henriksson 2011).

Pressure myography

Mouse mesenteric arteries were mounted in a pressure myograph system (120 CP, DMT A/S, Aarhus, Denmark) between two fire-polished glass pipettes with matching tip diameter (approx. 80 μm) for intraluminal perfusion and diameter measurement. The pressure myograph was placed on the stage of an inverted microscope (Olympus IX71; Olympus Danmark A/S, Ballerup, Denmark), and vessels were viewed through a 4X objective. The myograph chamber (5 mL) was continuously superfused (2 mL min^{-1}) with oxygenated (95% O_2 /5% CO_2) Krebs buffer, while arteries were being slowly pressurized and heated to 37 °C. To avoid bending of the artery at the maximal pressure of 120 mm Hg, the arteries were gently stretched to their approximate *in situ* length while maintaining the longitudinal force measurement between 0.1 and 0.35 mN. The luminal perfusion was blocked in the downstream direction to perform the measurements under no-flow conditions. It was checked that the pressure did not drop more than 1–2 mm Hg on the outflow side of the vessel to avoid vessels with side branches or leaks.

Subsequently, the pressure was gently lowered to 40 mm Hg, and after resting for 5–10 min, the artery was constricted with Krebs buffer containing 75 mM KCl (K75) for 3–5 min. After washout of K75 and resting for 5–10 min, the artery was again constricted for 3–5 min by adding 1 μM noradrenaline (NA) to the superfusate. Only arteries without leaks and showing a uniform constriction to K75 and NA were included in the study. Arteries included in the study were equilibrated with Krebs buffer at 80 mm Hg for 30–40 min before commencing the myogenic pressure step protocol. The control pressure curve was performed by changing the pressure between 20 and 120 mm Hg in 20 mm Hg increments while letting the artery constrict for 5 min at each pressure. After the control pressure curve was constructed, the artery was rested for 30 min before repeating the pressure protocol in the presence of 1 μM nifedipine. Finally, after the second pressure curve, the myograph chamber was superfused with Ca^{2+} -free Krebs' buffer + 2 mM EGTA for at least 10 min before repeating the pressure step protocol to obtain the passive pressure curve. During experiments, the outer diameter of the artery was measured using Myoview software (DMT A/S), and diameter, longitudinal force, temperature and pressure data were stored to a PC hard disk at 1 Hz. Offline analysis was used to calculate the mean steady-state diameters during the last 30 s at each pressure step. Mean diameters for K75 and NA measurements were measured at their steady-state diameter. There were no time-dependent diameter changes with K75 or NA after the steady-state diameter was reached.

Calcium imaging

The intracellular $[\text{Ca}^{2+}]$ measurements using Fura-PE3 ratiometric imaging of unpressurized mouse mesenteric terminal arterioles were performed at room temperature, as previously described (Jensen *et al.* 2004). The Ca^{2+} responses were evaluated as the peak Fura-PE3 Ratio to HB-PSS containing 60 mM KCl (K60). For each arteriole, normal HB-PSS was added first a couple of times to check for motion artifacts. Then, arterioles were challenged with K60 three times intermittently by washing steps for 5 min. Then arterioles were incubated with the Ca^{2+} antagonists for 10 min, followed by another series of challenges with K60. In most experiments, drugs were then washed away, and a third series of K60 challenge was performed.

Whole-cell patch clamp electrophysiology

Isolation of single VSMCs from mouse and rat mesenteric arteries (<200 μm) and the whole-cell patch clamp procedure was performed, as previously

published (Morita *et al.* 1999). In brief, short segments of the distal part of the isolated arteries were transferred to PSS with 1 mM Ca^{2+} and 0.5 mM papain (Worthington) and 0.5 mM 1,4-dithioerythritol (Sigma; Sigma-Aldrich Denmark ApS, Brøndby, Denmark), and incubated at 37 °C for 15 min, followed by transfer to 1 mM Ca^{2+} -containing PSS with 2 mM collagenase (type I; Worthington Biochemical Corp., Lakewood, NJ, USA) and incubated at 37 °C for 45 min. Single cells were dissociated by triturating the digested segments with a large-bore Pasteur pipette in Ca^{2+} -free PSS and stored at 4 °C until use. A low-noise, high-performance patch clamp amplifier (Axopatch 1D; Axon Instruments, Foster City, CA, USA) driven by a PC in conjunction with an A/D, D/A board (TL-1, Axon Instruments) was used to generate and apply voltage pulses to clamped cells and to record the corresponding membrane currents. Current signals were low-pass filtered at 1 kHz and digitized at 2 kHz before being stored to the PC hard disk. Linear leak subtraction was made using the hyperpolarizing P/4 or P/2 routine. Under the present experimental conditions, the series resistance of cells stayed almost constant throughout the experiment, and 50–70% of the series resistance was compensated. NNC 55-0396 was dissolved in water and added in increasing concentrations (10–10 μM) when steady-state inhibition was reached after approx. 100-s exposure. In initial experiments ($N = 3$) using only 1 μM NNC 55-0396 to block the total I_{Ba} , the remaining blocker-resistant current was totally abolished by the addition of Cd^{2+} (200 μM).

Immunofluorescence microscopy

Isolated second- and third-order mouse mesenteric arteries (3–5 from each mouse) were fixed in 2% paraformaldehyde dissolved in PBS for 1 h and subsequently cryo-protected in 30% sucrose for 2 h, or until they were submerged at the bottom of the sucrose solution. Cryo-protected arteries were embedded in Tissue-Tek®; Sakura Finetek Denmark ApS, Copenhagen, Denmark contained in a plastic mould and immediately quick-frozen in liquid nitrogen. Freeze sections (5 μm) were cut on a cryostat (Leica CM 1950) and collected on precleaned Superfrost Plus microscope slides (Thermo Scientific; Fisher Scientific GmbH, Schwerte, Germany). The immunostaining procedure was performed, as previously described (Jensen *et al.* 1999). In brief, frozen sections were left at room temperature for 1 h before they were hydrated 3 \times 5 min in PBS. Unspecific staining was blocked with 5% donkey serum in PBS for 50 min at RT. The primary $\text{Ca}_v3.1$ polyclonal antibody (gift from Dr. LL Cribbs, Loyola University, Ill.) was diluted 1 : 1500 in PBS and added to the sections for

90 min at RT or overnight at 4 °C. The specificity of the $\text{Ca}_v3.1$ antibody has previously been established (Rodman *et al.* 2005). The antigenic peptide sequence (FVCQGEDTRNITNKSDCAEAS) used for preabsorption experiments to verify the specificity of the antibody towards the $\text{Ca}_v3.1$ epitope was synthesized by United Peptide Corp. (Bethesda, MD, USA). In parallel preabsorption experiments, the primary antibody diluted in PBS was incubated with the antigenic peptide at 40–50 $\mu\text{g}/\text{mL}$ for 1 h at RT while shaking. The antibody–antigen mixture was vortexed and spun down shortly before applying it to the tissue sections and incubated as for primary antibody. In each experiment, a negative control with secondary antibody alone was also included. After incubation with primary antibody, the washing step consisted of wash with high-salt PBS for 5 min (to reduce non-specific staining) followed by normal PBS for 2 \times 5 min. Secondary antibody (1 : 800; Alexa Fluor® 488 Donkey anti-rabbit IgG, Molecular Probes; Life Technologies Europe BV, Nærum, Denmark) and Rhodamin-Phalloidin (1 : 400, Molecular Probes) were diluted in PBS and added for 60 min at RT. The washing step was repeated. Sections were treated with DAPI (0.1 $\mu\text{g}/\text{mL}$) in PBS for 30 min at RT. Finally, sections were covered with Immersion Liquid Type F (Leica), and cover slip was mounted for inspection. Sections were imaged with a Leica DM RB epifluorescence microscope through a Leica PL Fluotar oil-immersion objective (40X/1.00–0.50) using an external light source (EL 6000), digital camera (DFC 350 FX) and software (LAS Vers. 2.8.1) from Leica. For each experiment, all sections were imaged under identical microscope and camera settings. There was no visible staining in the negative controls using secondary antibody alone. Using Adobe Photoshop CS4, captured images were cropped, rotated, and the brightness and contrast were enhanced equally in sections incubated with primary antibody and primary antibody + peptide preincubation.

Quantitative real-time PCR (Q-PCR)

After dissection, second- and third-order branches of mouse mesenteric artery (3–4 from each mouse) were stored in RNeasy Lysis Buffer (Sigma) at 4 °C until used. Extraction of total RNA was performed using a RNeasy Lysis Buffer homogenizer and RNeasy Micro® kit (Qiagen; Qiagen GmbH, Hilden, Germany) according to the manufacturer's instruction. cDNA was produced from freshly extracted total RNA using a Promega kit according to the manufacturer's instruction. Both RT+ and RT– samples were prepared for each mouse. cDNA from mouse whole brain was prepared in the same way and used as a calibrator sample. Primers were picked using

Table 1 QPCR primers

Gene name	Forward primer (5'-3')	Reverse primer (5'-3')	Product size (BP)	Accession no.
Cacna1c	CGTTCTCATCCTGCTCAACA	GGTGTACCTCGGTGATTGCT	236	BC138031
Cacna1 h	CCTTTCTCAGCGTCTCCAAC	GCCACAATGATGTCAACCAG	169	BC138026
Cacna1a	TGCTGTGCTCACTGTTTTCC	TTCTCCACACGTTCCCTTTC	198	NM007578
Trpc1	GACATTCCAGGTTTCGTCTTG	GTCAGCACTAAGTTCAAACGC	107	NM011643
Trpc3	GATCGAGGATGACAGTGATGTAG	TCCATCATCGAAGTAGGAGAGC	73	NM019510
Trpc6	TACAATCTGGCCAGGATAAAAGTG	CACAGCGATTGCATAAAGACC	75	NM013838
Adra1a	ATTGTGGTGGGATGCTTCGT	ACTGTTTCCGGTGGCTTGAA	95	NM013461
Adra1b	GCCAAAACCTTGGGCATTGT	AAGTAGCCAGCCAGAACAC	140	NM007416
Adra1d	CAAGACCCTAGCCATCGTCG	GAAGACGCCCTCTGATGGTT	112	NM013460
Actb	AGCCATGTACGTAGCCATCC	CTCTCAGCTGTGGTGGTGAA	228	NM007393

Primer Blast or Primer 3 (see Table 1). A Blast search confirmed that the primers did not contain perfect matches to unintended targets. Conventional PCR using mouse cDNA and intron-spanning primers did not reveal any genomic DNA contamination. Q-PCR was performed using a LightCycler 480[®] apparatus (Roche; Roche Diagnostics A/S, Hvidovre, Denmark) and SYBR[®] Green PCR Master Mix. The standard Q-PCR cycle protocol was annealing at 60 °C for 10 s, and elongation at 72 °C for 20 s. Production of a standard curve for each primer pair using calibrator cDNA showed efficiencies in the range [1.83–2.10] and slopes in the range [–3.13 to –3.67]. The melting curve analyses revealed single peaks, only. For each primer pair, the amplified product was of the expected size, and the RT– and H₂O-loaded negative controls did not reveal any amplification. The reference gene β -actin (rActB) expression did not vary significantly between samples.

Solutions and chemicals

Krebs Buffer contained the following concentrations of salts (mM): NaCl 118; KCl 4.7; MgSO₄ 1.2; CaCl₂ 2; NaHCO₃ 25; KH₂PO₄ 1.2. In the Krebs buffer with 75 mM KCl (K75), NaCl was substituted with equimolar amounts of KCl. In the Ca²⁺-free Krebs buffer, CaCl₂ was replaced with 2 mM EGTA. Hepes-buffered physiological saline solution (HB-PSS) contained the following concentrations of salts (mM): NaCl 140; KCl 5; MgCl₂ 1.2; CaCl₂ 2; Hepes 10. In the HB-PSS with 60 mM KCl (K60), NaCl was substituted with equimolar amounts of KCl. A HB-PSS without CaCl₂ (no EGTA) was used during the mounting procedure of small arteries in pressure myograph experiments. Phosphate-buffered saline solution (PBS) contained (mM): NaCl 137; KCl 2.7 Na₂HPO₄ 10; KH₂PO₄ 1.76. In high-salt PBS (HS-PBS), the concentration of NaCl was increased to 411 mM. Glucose (5 mM) was added to each buffer (except PBS) immediately before use. pH was adjusted to 7.4 by equilibration with 5% CO₂

for Krebs buffer(s), and by adding 1 N NaOH for HB-PSS, PBS and HS-PBS. For whole-cell patch clamp experiments, a HB-PSS was used as bath solution, except that 5 mM BaCl₂ replaced Ca²⁺ as charge carrier and that pH was adjusted to 7.4 with Tris base. The pipette (internal) Cs⁺ solution contained (in mM) Cs⁺ 140, Mg²⁺ 2.0, Cl[–] 144, Phospho-creatine 5, Na₂ATP 1, EGTA 10 and HEPES 10 (adjusted to pH 7.2 with Tris base). Nifedipine, NNC 55-0396, NiCl₂, BaCl₂, CdCl₂, Pluronic F-127, Cremophore EL, DAPI and all other salts and chemicals were from Sigma Aldrich Co.

Statistics

Data were presented as raw data or mean \pm SEM with statistical significance tested using Student's *t*-test, except for Fig. 2a,b where the Control and Nifedipine pressure curves were evaluated versus the passive curves using a two-way repeated measures ANOVA with Bonferroni post-test for comparing individual pressure levels (multiple comparisons). A *P*-value of <0.05 was considered statistically significant. In Fig. 3b, the pharmacological effects were calculated as the increase from baseline Fura-PE3 R to K60 exposure (ΔR) before and after addition of Ca²⁺ channel blockers and expressed as the % remaining Ca²⁺ entry in mesenteric arterioles during drug exposure according to: $(\Delta R_{\text{drug}}/\Delta R_{\text{control}})*100$. The vasoconstriction to K75 and NA in mouse mesenteric artery was expressed as the difference in % vascular tone $(PD - AD/PD)*100$ between the resting diameter in normal Krebs buffer and Krebs buffer with high KCl or NA. Concentration-inhibition curves for NNC 55-0396 on I_{Ba} and NI-I_{Ba} were analysed by fitting data points averaged from 4 cells by the Hill equation for estimation of the 50% inhibitory concentration (IC₅₀) and Hill coefficient (n_H), respectively. Q-PCR data were evaluated either as Ratios of target gene to ActB cycle thresholds (*C_t*-values) in small mesenteric artery samples, or using the $2^{-\Delta\Delta C_t}$ method of normalized

relative ratios (Livak & Schmittgen 2001). The latter was calculated by the formula: Normalized relative ratio = $2^{-\Delta\Delta C_t}$, where $\Delta C_t = C_t$ (target) – C_t (rActB), and $\Delta\Delta C_t = \Delta C_t$ (sample) – ΔC_t (calibrator). The two calculation methods yielded similar results and statistical significance.

Results

We initially investigated by indirect immunofluorescence microscopy the expression and localization of Cav3.1 T-type Ca^{2+} channels in mouse mesenteric artery. As shown in a cross-section of an artery in Fig. 1 (Panel A), the green Cav3.1 staining is abundant in the arterial wall. Cav3.1 expression was not detectable in ECs, because the nuclei of ECs (*white arrows*) facing the lumen of the vessel are not covered by green Cav3.1 staining. In the longitudinal section through the *tunica media* (Panel C), it is clearly shown that Cav3.1 staining is abundant in VSMCs. We confirmed the specificity of the primary antibody for the Cav3.1 epitope by showing that the green staining is absent in sections of the same arteries labelled with primary antibody preincubated with its antigenic peptide (Panels B and D). Taken together, this expression

pattern of Cav3.1 is consistent with our previous findings in rat mesenteric arterioles and small arteries (Braunstein *et al.* 2009).

We hypothesized that a Cav3.1 T-type channel window current could be involved in maintenance of myogenic tone at low pressures associated with relatively small myogenic depolarization in mouse mesenteric arteries. This was investigated by pressure myograph experiments in which the steady-state constriction to intraluminal pressures in the range from 20 to 120 mm Hg was recorded. As shown in Fig. 2a, arteries from age-matched wild-type mice were significantly constricted in the pressure range from 40 to 120 mm Hg in the control situation with Krebs buffer compared with the passive situation where the vessels were exposed to Ca^{2+} -free solution. In the wild-type mice, a concentration of nifedipine (1 μM) sufficient to abolish all L-type channels expressed in smooth muscle (Morel *et al.* 1998), resulted in a pressure curve that was not significantly different from the passive curve, except at low pressure (40 mm Hg). This indicated that a non-L-type Ca^{2+} channel might be important at low pressure. Interestingly, in arteries from Cav3.1^{−/−} mice, the myogenic tone was abolished at low pressures from 40 to 80 mm Hg, whereas the

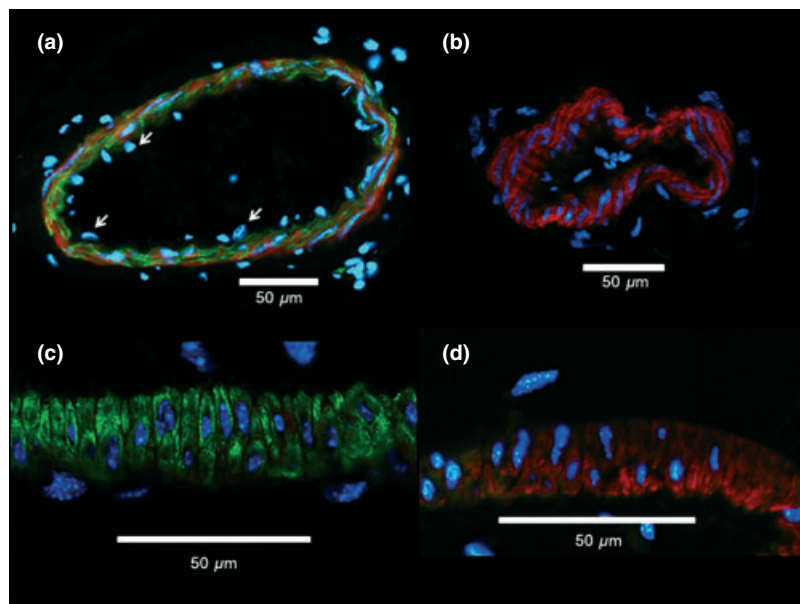


Figure 1 Immunolocalization of Cav3.1 protein (green staining) in mouse small mesenteric artery. Red colour represents smooth muscle α -actin staining and blue colour represents nuclei. (a) cross-section of an artery showing labelling of Cav3.1 in the vascular wall. Note the absence of green staining around EC nuclei (white arrows). (b) Cross-section of the same artery stained with primary Cav3.1 antibody preincubated with its antigenic peptide. Note the absence of green Cav3.1 staining in this arterial section. (c) Longitudinal section through the *tunica media* in mouse mesenteric artery. Individual vascular smooth muscle cells (VSMCs) labelled with green Cav3.1 staining are clearly distinguished. (d) Longitudinal section through the *tunica media* of mesenteric artery incubated under similar conditions with primary antibody + antigenic peptide. Note the suppression of green staining in VSMCs in this artery. Images in (a) vs. (b) and (c) vs. (d) were captured under identical camera and microscope settings. Images are representative of staining in at least 3 different wild-type mice.

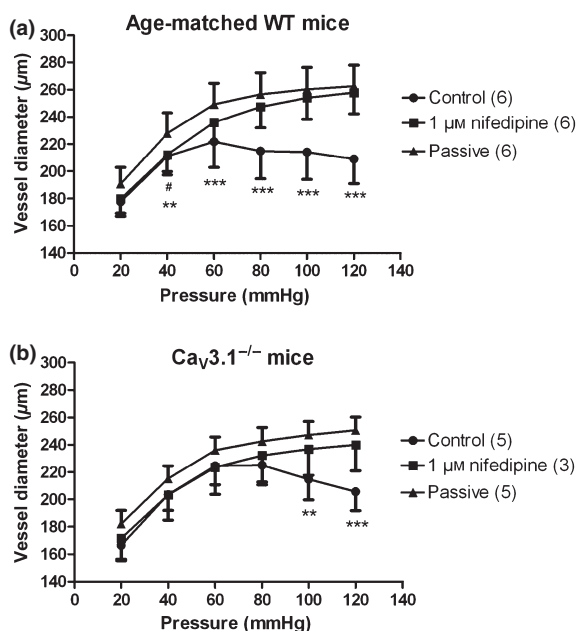


Figure 2 Myogenic response in small mesenteric artery of wild-type and $\text{Ca}_v3.1^{-/-}$ mice. (a) Control pressure curve shows diameter of artery when superfused with normal Krebs buffer. Nifedipine was used in the Krebs buffer to block all L-type channels. The passive pressure curve was obtained by superfusing arteries with a Ca^{2+} -free (+EGTA) Krebs buffer. Note the development of myogenic tone at pressures from 40 to 120 mm Hg seen as a significant constriction compared with the passive curve. Note that nifedipine did not significantly block the myogenic tone at 40 mm Hg. (b) Myogenic tone under control condition is not significant at pressures from 20 to 80 mm Hg. Nifedipine abolishes myogenic tone at 100 to 120 mm Hg. (** $P < 0.01$ control *vs.* passive diameter; *** $P < 0.001$ control *vs.* passive diameter; # $P < 0.05$ in nifedipine-treated *vs.* passive diameter). The number of vessels/animals is shown in brackets.

arterial diameter and myogenic tone at 100 and 120 mm Hg were similar to the age-matched wild-type mice (Fig. 2b). These data strongly suggest that in wild-type mouse mesenteric artery, $\text{Ca}_v3.1$ T-type channels are involved in the maintenance of myogenic tone at low pressures up to 80 mm Hg, that $\text{Ca}_v3.1$ channels are inactivated at high pressures of 100–120 mm Hg, and that the L-type channels are strongly activated in this pressure range.

In previous studies, it has been suggested that a splice variant of T-type channels is expressed in mesenteric resistance vessels and contribute to sustained Ca^{2+} entry at membrane potentials normally found in VSMCs (Jensen & Holstein-Rathlou 2009). To investigate this possibility, we compared the Ca^{2+} entry and vasoconstriction to high KCl in age-matched wild-type and $\text{Ca}_v3.1^{-/-}$ mice. As shown in Fig. 3a, the Ca^{2+} increase to high KCl in mouse mesenteric

terminal arterioles ($<40 \mu\text{m}$) was similar in wild-type and $\text{Ca}_v3.1$ -deficient mice. Furthermore, the vasoconstriction measured as the increase in vascular tone from baseline to high KCl (ΔTone) in small mesenteric arteries ($<200 \mu\text{m}$) was also similar in wild-type and $\text{Ca}_v3.1$ -deficient mice (Fig. 3c). These data clearly show that $\text{Ca}_v3.1$ channels are not involved in the nifedipine-insensitive responses to high-voltage activation with KCl. How does this comply with the pronounced effects of NNC 55-0396, which was recently shown to potently inhibit recombinantly expressed $\text{Ca}_v3.1$ channels with no effect on high-voltage-activated Ca^{2+} currents (Huang *et al.* 2004). To investigate this, we next tested the pharmacology of KCl-induced Ca^{2+} entry in mesenteric arterioles from $\text{Ca}_v3.1^{-/-}$ mice (Fig. 3b). About 40% of the Ca^{2+} entry was insensitive to nifedipine, and when adding the $\text{Ca}_v3.2$ -specific blocker NiCl_2 (30 μM) on top of nifedipine, there was no further inhibition of the Ca^{2+} entry. These data show that neither $\text{Ca}_v3.1$ nor $\text{Ca}_v3.2$ T-type Ca^{2+} channels mediate nifedipine-insensitive Ca^{2+} entry to KCl. Furthermore, NNC 55-0396 (10 μM), irrespective of whether it was added on top of nifedipine or NiCl_2 , abolished all Ca^{2+} entry to high KCl in mesenteric arterioles from $\text{Ca}_v3.1$ -deficient mice. These data clearly demonstrate that NNC 55-0396 is not a specific T-type channel blocker.

The question still remained whether NNC 55-0396 can be used to distinguish between high-voltage-activated Ca^{2+} channels of the L-type *vs.* non-L-type in native mesenteric artery VSMCs. To investigate this further, we tested the effects of NNC 55-0396 on high-voltage-activated whole-cell barium (Ba^{2+}) currents (I_{Ba}) before or after addition of 10 μM nifedipine to block all L-type channel activity. Fig. 4a,b show original recording and mean Ba^{2+} currents found in mouse mesenteric VSMCs. It is seen that the total I_{Ba} is activated by stepping from a holding potential of -80 mV to depolarized potentials in the range from -30 mV to $+60 \text{ mV}$ with a peak of the I/V-curve at 0 to $+10 \text{ mV}$. The current remaining after addition of nifedipine ($\text{NI-}I_{\text{Ba}}$) amounted to approx. 20% of the total I_{Ba} . As the Ba^{2+} currents in mouse VSMCs were rather small, we continued investigating the effects of NNC 55-0396 in rat mesenteric artery VSMCs. In Fig. 5a–c is shown that NNC 55-0396 dose dependently blocks both total I_{Ba} and $\text{NI-}I_{\text{Ba}}$ in rat mesenteric artery VSMC with IC_{50} values of 0.59 μM and 0.96 μM , respectively. These data clearly show that NNC 55-0396 blocks high-voltage-activated Ca^{2+} channels of both L-type and non-L-type with similar high potency and should therefore not be used in native VSMCs to distinguish between different high-voltage-activated Ca^{2+} channels.

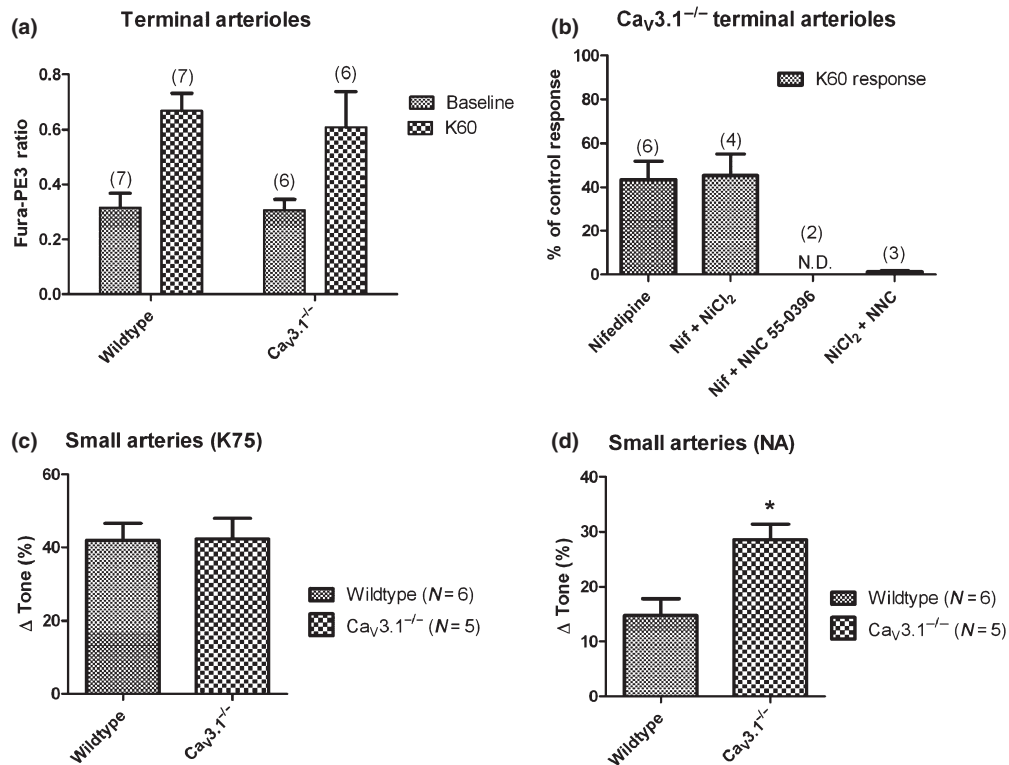


Figure 3 (a) Measurements of intracellular Ca^{2+} increase (Fura-PE3 Ratio) to high KCl (60 mM) in mesenteric terminal arterioles ($<40 \mu\text{m}$) from wild-type and $\text{Ca}_v3.1$ -deficient mice. (b) Remaining Ca^{2+} increase (% of control response) to K60 in terminal arterioles from $\text{Ca}_v3.1^{-/-}$ mice during exposure to L-type channel inhibitor nifedipine (10 μM), $\text{Ca}_v3.2$ T-type Ca^{2+} channel inhibitor NiCl_2 (30 μM) and putative T-type channel blocker NNC 55-0396 (10 μM). N.D. = not detectable. (c, d) Vasoconstriction (Δ Tone) to high KCl (75 mM) and noradrenaline (1 μM) in mesenteric small arteries ($<200 \mu\text{m}$) pressurized to 40 mm Hg. The number of vessels/animals is shown in brackets.

We also tested the vasoconstrictor effects of a submaximal concentration of noradrenaline (NA 1 μM) in mouse small mesenteric arteries pressurized at 40 mm Hg. Surprisingly, NA elicited a significantly stronger vasoconstriction (increase in vascular tone from baseline) in mice deficient in the $\text{Ca}_v3.1$ channel than in age-matched wild-type mice (Fig. 3d). We speculated that this could be due to an upregulation in the expression of different Ca^{2+} handling proteins and therefore tested by Q-PCR the mRNA expression of several isoforms of voltage-gated Ca^{2+} channel, transient receptor potential subfamily C, and α_1 -adrenergic receptor in mouse small mesenteric arteries. As shown in Table 2, these Ca^{2+} handling proteins were not differentially expressed in mesenteric arteries from age-matched wild-type mice and $\text{Ca}_v3.1$ -deficient mice.

Discussion

The involvement of T-type channels in the regulation of arteriolar tone has long been controversial for several reasons. Firstly, the membrane potentials at which

the T-type channels are activated and inactivated are more hyperpolarized than what has been measured in VSMCs of pressurized arteries and arterioles (Perez-Reyes 2003, Jensen & Holstein-Rathlou 2009). Secondly, despite the fact that many studies have shown the existence of a non-L-type Ca^{2+} channel, which contributes to arteriolar tone in mesenteric, cremasteric, renal and cerebral vessels (Gustafsson *et al.* 2001, Hansen *et al.* 2001, Morita *et al.* 2002, VanBavel *et al.* 2002, Jensen *et al.* 2004, Kuo *et al.* 2010), these studies have relied on mibefradil and other non-specific T-type channel blockers with a known effect on high-voltage-activated Ca^{2+} channels (Bezprozvanny & Tsien 1995, Aczel *et al.* 1998, Jimenez *et al.* 2000, Moosmang *et al.* 2006). In an attempt to clarify the contribution of T-type channels to arteriolar tone regulation, we employed mice deficient in the $\text{Ca}_v3.1$ subtype of T-type channels and tested the three following hypotheses: (i) Do $\text{Ca}_v3.1$ T-type channels contribute to myogenic tone at low arterial pressure, under which the membrane potential of VSMCs in pressurized arteries was previously measured to be in the range from -60 to -50 mV (Knot & Nelson 1998,

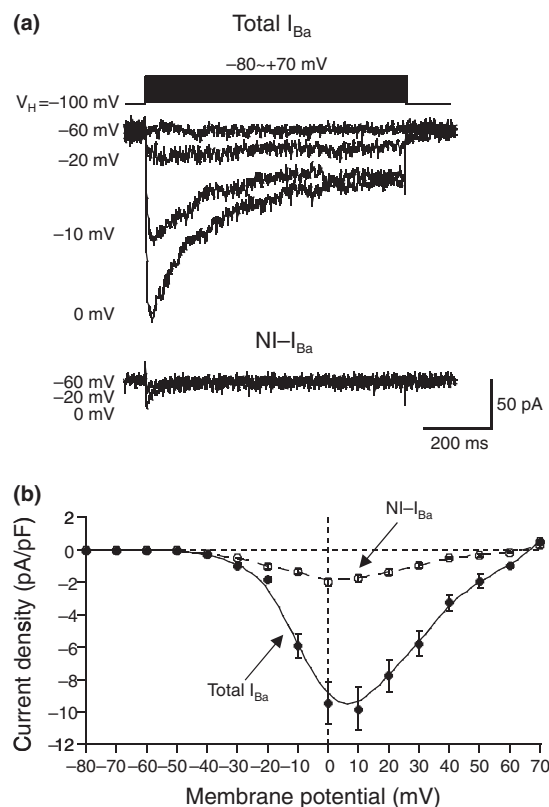


Figure 4 Current–voltage (I - V) relationships of total barium current (total I_{Ba}) and nifedipine- ($10\ \mu\text{M}$) insensitive barium current ($\text{NI-}I_{\text{Ba}}$) in mouse mesenteric artery myocytes. (a) Representative traces of total I_{Ba} and $\text{NI-}I_{\text{Ba}}$ (with $5\ \text{mM}\ \text{Ba}^{2+}$ as charge carrier). (b) I - V relationships of total I_{Ba} and $\text{NI-}I_{\text{Ba}}$ ($n = 4$ each). Current amplitudes (pA) were normalized by cell capacitances (pF).

Kotecha & Hill 2005). (ii) Do $\text{Ca}_v3.1$ T-type channels partially mediate Ca^{2+} influx and vasoconstriction to high-voltage activation using high KCl concentration in mouse mesenteric arteries ($<200\ \mu\text{m}$) and arterioles ($<40\ \mu\text{m}$)? (iii) Is NNC 55-0396 a specific T-type channel blocker?

With respect to the first hypothesis, it was clearly shown that the myogenic tone in $\text{Ca}_v3.1^{-/-}$ mice was abolished in the pressure range from 40 to 80 mm Hg, as compared with age-matched wild-type mice (Fig. 2). We did not measure the membrane potential of pressurized mouse mesenteric arteries to confirm that it was in the range required for sustained activation of $\text{Ca}_v3.1$ channels through window currents. However, our data indicate that L-type channels were not crucial for myogenic tone at low arterial pressure, because nifedipine ($1\ \mu\text{M}$) was ineffective at blocking myogenic tone at 40 mm Hg in the wild-type mice. Furthermore, the fact that the myogenic response at 100–120 mm Hg was very powerful in $\text{Ca}_v3.1^{-/-}$ mice and constricted the arteries to attain the same diameter as in the

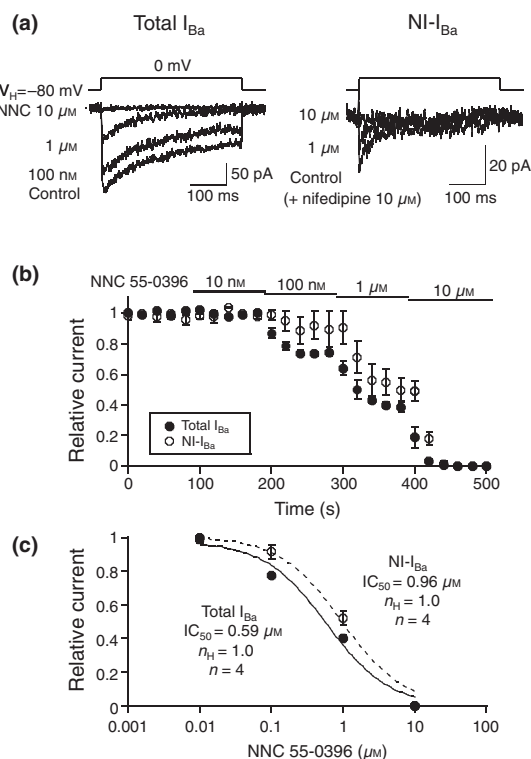


Figure 5 Effects of NNC 55-0396 on total barium current (total I_{Ba}) and nifedipine- ($10\ \mu\text{M}$) insensitive barium current ($\text{NI-}I_{\text{Ba}}$) of rat mesenteric artery myocytes. (a) Representative traces of inhibitory effect of NNC 55-0396 on total I_{Ba} and $\text{NI-}I_{\text{Ba}}$ (with $5\ \text{mM}\ \text{Ba}^{2+}$ as charge carrier). (b) Effects of NNC 55-0396 on I_{Ba} and $\text{NI-}I_{\text{Ba}}$ ($n = 4$ each). All points were standardized by the initial current at time zero. Total I_{Ba} and $\text{NI-}I_{\text{Ba}}$ were indicated by filled circles and open circles, respectively. (c) Concentration–inhibition curves for NNC 55-0396 on I_{Ba} and $\text{NI-}I_{\text{Ba}}$. All points were averaged from 4 cells and fitted by Hill equation. IC_{50} ; 50% inhibitory concentration, n_H ; Hill coefficient. All data are expressed as mean \pm SEM.

wild-type mice, suggests that the mechanosensor involved in the development of spontaneous myogenic tone is intact in mice deficient in the $\text{Ca}_v3.1$ channels. In addition, nifedipine ($1\ \mu\text{M}$) was effective in blocking myogenic tone at 100–120 mm Hg in wild-type and $\text{Ca}_v3.1^{-/-}$ mice, which lends further support to the notion that L-type channels are crucial for maintenance of myogenic tone at high arterial pressure. The role of $\text{Ca}_v3.1$ channels in myogenic tone is supported by the presence of the $\text{Ca}_v3.1$ protein in the smooth muscle layer of mouse mesenteric arteries (Fig. 1). It is therefore suggested that $\text{Ca}_v3.1$ channels are activated and contribute to myogenic tone at low arterial pressure and that they are inactivated at high arterial pressure where L-type channel activation is responsible for the maintenance of myogenic tone. It remains to be established whether T-type channels are important for basal tone *in vivo*, but as the pressure in mesenteric

Table 2 Q-PCR data

Target gene	Protein symbol	WT mice: target gene expression (N)	Ca _v 3.1 ^{-/-} mice: target gene expression (N)	P-value (t-test)
Cacna1c	Ca _v 1.2 (L-type)	0.225 ± 0.052 (7)	0.231 ± 0.037 (6)	0.93
Cacna1 h	Ca _v 3.2 (T-type)	0.202 ± 0.024 (7)	0.155 ± 0.049 (6)	0.39
Cacna1a	Ca _v 2.1 (P/Q-type)	0.024 ± 0.003 (7)	0.034 ± 0.010 (3)	0.26
Trpc1	TRPC1	0.177 ± 0.011 (7)	0.181 ± 0.022 (3)	0.87
Trpc3	TRPC3	0.078 ± 0.017 (7)	0.051 ± 0.025 (3)	0.41
Trpc6	TRPC6	0.137 ± 0.017 (7)	0.149 ± 0.022 (6)	0.66
Adra1a	α _{1A} -R	0.363 ± 0.028 (7)	0.279 ± 0.064 (3)	0.32
Adra1b	α _{1B} -R	0.020 ± 0.003 (7)	0.024 ± 0.008 (3)	0.67
Adra1d	α _{1D} -R	0.102 ± 0.013 (7)	0.077 ± 0.012 (3)	0.20

Normalized mRNA expression data are presented as 2^{-ΔΔC_T}-value (see Methods). N equals the number of mice studied. For each mouse studied, RNA from three to four small mesenteric arteries was pooled and used for the Q-PCR analysis.

arteries in conscious rats was in the range from 60 to 80 mm Hg (Fenger-Gron *et al.* 1995), we suggest that T-type channels may to some extent contribute to the basal tone under resting conditions.

Our finding that the noradrenergic tone measured at 40 mm Hg in mesenteric arteries was augmented in Ca_v3.1^{-/-} mice compared with their wild-type controls (Fig. 3d) deserves attention. None of the Ca²⁺ channels, TRPC channels or α₁-adrenergic receptor subtypes present in mouse mesenteric arteries were differentially expressed at the mRNA level in the wild-type vs. knockout animals (Table 2). Although we cannot be sure that these channels and receptors are not upregulated at the protein level in the Ca_v3.1^{-/-} mice, our data suggest that the augmented noradrenergic tone is not explained by a simple upregulation of these mechanisms. However, the increase in noradrenergic tone could be a natural compensation for mice born with a deletion of the Ca_v3.1 channels, as the myogenic tone was abolished at the lower arterial pressures, which would necessitate a secondary mechanism to compensate for the loss in vascular tone. Furthermore, the Ca_v3.1^{-/-} animals are bradycardic, due to a slowing of the sinoatrial node pacemaker rhythm and the A-V conduction, but they have normal mean arterial blood pressure (Mangoni *et al.* 2006). It is tempting to speculate that the noradrenaline sensitivity of the resistance vessels is upregulated in Ca_v3.1^{-/-} animals to increase the peripheral resistance enough to keep the animals normotensive under resting conditions.

With respect to the second hypothesis, our data clearly showed that KCl-induced Ca²⁺ entry and vasoconstriction in mesenteric arteries and arterioles was not different in wild-type and Ca_v3.1-deficient mice (Fig. 3a,c). Furthermore, the nifedipine-insensitive Ca²⁺ increase to high KCl in arterioles from Ca_v3.1^{-/-} animals was not sensitive to a low concentration of Ni²⁺ (30 μM), which is considered to be specific for Ca_v3.2 channels (Fig. 3b). Taken together, our data from the

wild-type and knockout mice clearly shows that Ca_v3.1 and Ca_v3.2 T-type Ca²⁺ channels do not mediate depolarization-induced Ca²⁺ entry and vasoconstriction to high KCl. We must assume that this is due to the fact that the depolarization induced by high KCl is so large that the T-type channels are inactivated. This conclusion is supported by a patch clamp study in rat mesenteric artery VSMCs showing that nifedipine-insensitive whole-cell Ca²⁺ currents with T-type-like pharmacology was not reminiscent of recombinant Ca_v3.1 T-type Ca²⁺ channels expressed in HEK cells (Morita *et al.* 2002). Previous studies argue against the possibility of several high-voltage-activated Ca²⁺ channels as candidates for the nifedipine-insensitive Ca²⁺ entry pathway in mesenteric arteries and arterioles, because specific peptide toxins targeting P/Q-type, N-type, or R-type channels were not effective (Morita *et al.* 2002, Jensen *et al.* 2004). In addition, the mesenteric nifedipine-insensitive Ca²⁺ currents did not match those of recombinant Ca_v2.3 R-type channels expressed in HEK cells (Morita *et al.* 2002). One hypothetical explanation for our observations could be that depolarization *per se* triggers Ca²⁺ store release (Urena *et al.* 2007), and indirectly activates plasma membrane Ca²⁺ channels by emptying of these stores. However, the Ca²⁺ currents measured with Ba²⁺ as charge carrier in the presence of 10 μM nifedipine in mesenteric artery VSMCs (Morita *et al.* 1999, 2002) are not similar to any of the storage-operated Ca²⁺ permeable channels of the TRPC family, so the identity of the high-voltage-activated nifedipine-insensitive Ca²⁺ channel awaits further elucidation.

With respect to the third hypothesis, NNC 55-0396 potentially inhibited high-voltage-activated Ca²⁺ influx in Ca_v3.1^{-/-} mice and Ba²⁺ currents in the presence and absence of nifedipine with similar potency. These data are supported by a recent study in which 1 μM NNC 55-0396 abolished the total high-voltage-activated Ba²⁺ currents in rat basilar artery myocytes (Kuo *et al.*

2010). These findings demonstrate that NNC 55-0396, like its analogue mibefradil, cannot be considered as a specific T-type blocker in the concentration range from 1 to 10 μ M. It is therefore crucial for any study making use of mibefradil and its derivatives as well as any other putative T-type channel blocker, to perform the necessary positive and negative control experiments to verify the specificity of the drugs.

Conclusions

Our data using mice deficient in the Ca_v3.1 T-type channel represent new evidence for the involvement of non-L-type channels in arteriolar tone regulation. We showed that Ca_v3.1 channels are important for maintenance of myogenic tone at an arterial pressure in the range from 40–80 mm Hg, which is found under resting conditions *in vivo*. We also showed that, contrary to earlier findings in the literature, Ca_v3.1 channels are not involved in Ca²⁺ entry and vasoconstriction to large depolarization such as during stimulation with high KCl. Finally, we caution against using NNC 55-0396 as a specific T-type channel blocker in native cells expressing high-voltage-activated Ca²⁺ channels. A candidate for the non-L-type high-voltage-activated Ca²⁺ entry channel in mesenteric artery myocytes is still missing.

Conflicts of interest

The authors declare no conflicts of interest.

The Lundbeck Foundation and The A.P. Møller Foundation for the Advancement of Medical Science are gratefully acknowledged for financial support. The authors wish to express their gratitude to Dr. Leanne L. Cribbs for providing the Ca_v3.1 antibody and to Ms. Vibeke G. Christensen for expert technical assistance. The authors would like to thank the Stiftelsen Nordisk Fysiologi, SNF and the German Research Foundation (Deutsche Forschungsgemeinschaft, DFG) for their generous support for the AP Symposium on 'Hemodynamic Mechanisms in Acute Kidney Injury'.

References

Aczel, S., Kurka, B. & Hering, S. 1998. Mechanism of voltage- and use-dependent block of class A Ca²⁺ channels by mibefradil. *Br J Pharmacol* **125**, 447–454.

Ball, C.J., Wilson, D.P., Turner, S.P., Saint, D.A. & Beltrame, J.F. 2009. Heterogeneity of L- and T-channels in the vasculature: rationale for the efficacy of combined L- and T-blockade. *Hypertension* **53**, 654–660.

Beltrame, J.F., Turner, S.P., Leslie, S.L., Solomon, P., Freedman, S.B. & Horowitz, J.D. 2004. The angiographic and clinical benefits of mibefradil in the coronary slow flow phenomenon. *J Am Coll Cardiol* **44**, 57–62.

Bezprozvanny, I. & Tsien, R.W. 1995. Voltage-dependent blockade of diverse types of voltage-gated Ca²⁺ channels expressed in *Xenopus* oocytes by the Ca²⁺ channel antagonist mibefradil (Ro 40-5967). *Mol Pharmacol* **48**, 540–549.

Braunstein, T.H., Inoue, R., Cribbs, L., Oike, M., Ito, Y., Holstein-Rathlou, N.H. & Jensen, L.J. 2009. The role of L- and T-type channels in local and remote calcium responses in rat mesenteric terminal arterioles. *J Vasc Res* **46**, 138–151.

Catterall, W.A., Striessnig, J., Snutch, T.P. & Perez-Reyes, E. 2003. International Union of Pharmacology. XL. Compendium of voltage-gated ion channels: calcium channels. *Pharmacol Rev* **55**, 579–581.

Chen, C.C., Lamping, K.G., Nuno, D.W., Barresi, R., Prouty, S.J., Lavoie, J.L., Cribbs, L.L., England, S.K., Sigmund, C. D., Weiss, R.M., Williamson, R.A., Hill, J.A. & Campbell, K.P. 2003. Abnormal coronary function in mice deficient in α 1H T-type Ca²⁺ channels. *Science* **302**, 1416–1418.

Davis, M.J. & Hill, M.A. 1999. Signaling mechanisms underlying the vascular myogenic response. *Physiol Rev* **79**, 387–423.

Fenger-Gron, J., Mulvany, M.J. & Christensen, K.L. 1995. Mesenteric blood pressure profile of conscious, freely moving rats. *J Physiol* **488**(Pt 3), 753–760.

Fukumoto, Y., Yasuda, S., Ito, A. & Shimokawa, H. 2008. Prognostic effects of benidipine in patients with vasospastic angina: comparison with diltiazem and amlodipine. *J Cardiovasc Pharmacol* **51**, 253–257.

Furukawa, T., Miura, R., Honda, M., Kamiya, N., Mori, Y., Takeshita, S., Isshiki, T. & Nukada, T. 2004. Identification of R(-)-isomer of efonidipine as a selective blocker of T-type Ca²⁺ channels. *Br J Pharmacol* **143**, 1050–1057.

Gustafsson, F., Andreasen, D., Salomonsson, M., Jensen, B.L. & Holstein-Rathlou, N. 2001. Conducted vasoconstriction in rat mesenteric arterioles: role for dihydropyridine-insensitive Ca(2+) channels. *Am J Physiol Heart Circ Physiol* **280**, H582–H590.

Hansen, P.B., Jensen, B.L., Andreasen, D. & Skott, O. 2001. Differential expression of T- and L-type voltage-dependent calcium channels in renal resistance vessels. *Circ Res* **89**, 630–638.

Huang, L., Keyser, B.M., Tagmose, T.M., Hansen, J.B., Taylor, J. T., Zhuang, H., Zhang, M., Ragsdale, D.S. & Li, M. 2004. NNC 55-0396 [(1S,2S)-2-(2-(N-[(3-benzimidazol-2-yl)propyl]-N-methylamino)ethyl)-6-fluoro-1,2,3,4-tetrahydro-1-isopropyl-2-naphthyl cyclopropanecarboxylate dihydrochloride]: a new selective inhibitor of T-type calcium channels. *J Pharmacol Exp Ther* **309**, 193–199.

Jensen, L.J. & Holstein-Rathlou, N.H. 2009. Is there a role for T-type Ca²⁺ channels in regulation of vasomotor tone in mesenteric arterioles? *Can J Physiol Pharmacol* **87**, 8–20.

Jensen, L.J., Schmitt, B.M., Berger, U.V., Nsumu, N.N., Boron, W.F., Hediger, M.A., Brown, D. & Breton, S. 1999. Localization of sodium bicarbonate cotransporter (NBC) protein and messenger ribonucleic acid in rat epididymis. *Biol Reprod* **60**, 573–579.

Jensen, L.J., Salomonsson, M., Jensen, B.L. & Holstein-Rathlou, N.H. 2004. Depolarization-induced calcium influx in rat

- mesenteric small arterioles is mediated exclusively via mibefradil-sensitive calcium channels. *Br J Pharmacol* 142, 709–718.
- Jimenez, C., Bourinet, E., Leuranguer, V., Richard, S., Snutch, T.P. & Nargeot, J. 2000. Determinants of voltage-dependent inactivation affect Mibefradil block of calcium channels. *Neuropharmacology* 39, 1–10.
- Kim, D., Song, I., Keum, S., Lee, T., Jeong, M.J., Kim, S.S., McEnery, M.W. & Shin, H.S. 2001. Lack of the burst firing of thalamocortical relay neurons and resistance to absence seizures in mice lacking alpha(1G) T-type Ca(2+) channels. *Neuron* 31, 35–45.
- Knot, H.J. & Nelson, M.T. 1998. Regulation of arterial diameter and wall [Ca²⁺] in cerebral arteries of rat by membrane potential and intravascular pressure. *J Physiol* 508(Pt 1), 199–209.
- Koh, K.K., Quon, M.J., Lee, S.J., Han, S.H., Ahn, J.Y., Kim, J.A., Chung, W.J., Lee, Y. & Shin, E.K. 2007. Efonidipine simultaneously improves blood pressure, endothelial function, and metabolic parameters in nondiabetic patients with hypertension. *Diabetes Care* 30, 1605–1607.
- Kotecha, N. & Hill, M.A. 2005. Myogenic contraction in rat skeletal muscle arterioles: smooth muscle membrane potential and Ca(2+) signaling. *Am J Physiol Heart Circ Physiol* 289, H1326–H1334.
- Kuo, I.Y., Ellis, A., Seymour, V.A., Sandow, S.L. & Hill, C. E. 2010. Dihydropyridine-insensitive calcium currents contribute to function of small cerebral arteries. *J Cereb Blood Flow Metab* 30, 1226–1239.
- Liao, P., Yu, D., Li, G., Yong, T.F., Soon, J.L., Chua, Y.L. & Soong, T.W. 2007. A smooth muscle Cav1.2 calcium channel splice variant underlies hyperpolarized window current and enhanced state-dependent inhibition by nifedipine. *J Biol Chem* 282, 35133–35142.
- Livak, K.J. & Schmittgen, T.D. 2001. Analysis of relative gene expression data using real-time quantitative PCR and the 2(-Delta Delta C(T)) Method. *Methods* 25, 402–408.
- Mangoni, M.E., Traboulsie, A., Leoni, A.L., Couette, B., Marger, L., Le, Q.K., Kupfer, E., Cohen-Solal, A., Vilar, J., Shin, H.S., Escande, D., Charpentier, F., Nargeot, J. & Lory, P. 2006. Bradycardia and slowing of the atrioventricular conduction in mice lacking Cav3.1/alpha1G T-type calcium channels. *Circ Res* 98, 1422–1430.
- Monteil, A., Chemin, J., Bourinet, E., Mennessier, G., Lory, P. & Nargeot, J. 2000. Molecular and functional properties of the human alpha(1G) subunit that forms T-type calcium channels. *J Biol Chem* 275, 6090–6100.
- Moosmang, S., Schulla, V., Welling, A., Feil, R., Feil, S., Wegener, J.W., Hofmann, F. & Klugbauer, N. 2003. Dominant role of smooth muscle L-type calcium channel Cav1.2 for blood pressure regulation. *EMBO J* 22, 6027–6034.
- Moosmang, S., Haider, N., Bruderl, B., Welling, A. & Hofmann, F. 2006. Antihypertensive effects of the putative T-type calcium channel antagonist mibefradil are mediated by the L-type calcium channel Cav1.2. *Circ Res* 98, 105–110.
- Morel, N., Buryi, V., Feron, O., Gomez, J.P., Christen, M.O. & Godfraind, T. 1998. The action of calcium channel blockers on recombinant L-type calcium channel alpha1-subunits. *Br J Pharmacol* 125, 1005–1012.
- Morita, H., Cousins, H., Onoue, H., Ito, Y. & Inoue, R. 1999. Predominant distribution of nifedipine-insensitive, high voltage-activated Ca²⁺ channels in the terminal mesenteric artery of guinea pig. *Circ Res* 85, 596–605.
- Morita, H., Shi, J., Ito, Y. & Inoue, R. 2002. T-channel-like pharmacological properties of highvoltage-activated, nifedipine-insensitive Ca(2+) currents in the rat terminal mesenteric artery. *Br J Pharmacol* 137, 467–476.
- Nelson, M.T., Patlak, J.B., Worley, J.F. & Standen, N.B. 1990. Calcium channels, potassium channels, and voltage dependence of arterial smooth muscle tone. *Am J Physiol* 259, C3–C18.
- Oshima, T., Ozono, R., Yano, Y., Higashi, Y., Teragawa, H., Miho, N., Ishida, T., Ishida, M., Yoshizumi, M. & Kambe, M. 2005. Beneficial effect of T-type calcium channel blockers on endothelial function in patients with essential hypertension. *Hypertens Res* 28, 889–894.
- Perez-Reyes, E. 2003. Molecular physiology of low-voltage-activated t-type calcium channels. *Physiol Rev* 83, 117–161.
- Persson, P.B. & Henriksson, J. 2011. Good publication practice in physiology. *Acta Physiol* 203, 403–407.
- Pratt, P.F., Bonnet, S., Ludwig, L.M., Bonnet, P. & Rusch, N.J. 2002. Upregulation of L-type Ca²⁺ channels in mesenteric and skeletal arteries of SHR. *Hypertension* 40, 214–219.
- Rodman, D.M., Reese, K., Harral, J., Fouty, B., Wu, S., West, J., Hoedt-Miller, M., Tada, Y., Li, K.X., Cool, C., Fagan, K. & Cribbs, L. 2005. Low-voltage-activated (T-type) calcium channels control proliferation of human pulmonary artery myocytes. *Circ Res* 96, 864–872.
- Sasaki, H., Saiki, A., Endo, K., Ban, N., Yamaguchi, T., Kawana, H., Nagayama, D., Ohhira, M., Oyama, T., Miyashita, Y. & Shirai, K. 2009. Protective effects of efonidipine, a T- and L-type calcium channel blocker, on renal function and arterial stiffness in type 2 diabetic patients with hypertension and nephropathy. *J Atheroscler Thromb* 16, 568–575.
- Urena, J., del Valle-Rodriguez, A. & Lopez-Barneo, J. 2007. Metabotropic Ca²⁺ channel-induced calcium release in vascular smooth muscle. *Cell Calcium* 42, 513–520.
- VanBavel, E., Sorop, O., Andreasen, D., Pfaffendorf, M. & Jensen, B.L. 2002. Role of T-type calcium channels in myogenic tone of skeletal muscle resistance arteries. *Am J Physiol Heart Circ Physiol* 283, H2239–H2243.
- Velat, G.J., Kimball, M.M., Mocco, J.D. & Hoh, B.L. 2011. Vasospasm after aneurysmal subarachnoid hemorrhage: review of randomized controlled trials and meta-analyses in the literature. *World Neurosurg* 76, 446–454.